SIMULATION OF THE UPGRADED PHOTOINJECTOR FOR THE 10 KW JLAB IR-FEL*

P. Piot, Department of Physics, Northern Illinois University, DeKalb, IL 60115, U.S.A.
and Accelerator Physics Center, Fermi National Accelerator Laboratory, Batavia, IL 60510, U.S.A.
D. Mihalcea, Department of Physics, Northern Illinois University, DeKalb, IL 60115, U.S.A.
C. Hernandez-Garcia, S. Zhang, Free-Electron Laser Group,
Thomas Jefferson Accelerator Laboratory, Newport News, VA 23606, U.S.A.

Abstract

The photoinjector of the JLab 10 kW IR FEL was recently upgraded: a new photocathode drive laser was commissioned and the booster section was replaced with new 5-cell cavities. In this paper we present numerical simulation and optimization of the photoinjector performances using ASTRA, IMPACT-T and IMPACT-Z beam dynamics codes. We perform these calculations for the nominal 350 keV operating voltage of the dc gun.

INTRODUCTION

Jefferson Lab is currently operating a high average power infrared free-electron laser [1]. The driver accelerator is an upgraded version of the now decommissioned 1 kW IR-Demo FEL [2]. The facility also serve as a platform to explore beam dynamics phenomena and technologies associated with the realization of very high-average-power free-electron lasers. The driver accelerator comprises a $\sim$ 10 MeV injector followed by a 80-200 MeV energy recovering superconducting RF linac that allows high average current operation with modest klystron power. To reach the 10 kW goal, the charge-per-bunch was increased from 60 pC to 135 pC and the bunch repetition rate from 37.425 MHz to 74.850 MHz. The requirements on beam quality at the wiggler location to lase with a 10 kW average power using 135 pC bunches are gathered in Table 1. The photoemission injector, whose block diagram is shown in Figure 1, is a key element in achieving the required beam quality. It basically consists of a 350 keV line coupled with a high gradient RF structure consisting of two CEBAF-type superconducting cavities that can accelerate the beam up to approximately 10 MeV. The accelerating section is followed by a 10 MeV injection line that includes a diagnostics suite.

BEAM GENERATION & ACCELERATION

The low-energy line consists of a high-voltage DC photoemission gun for electron generation, a room-temperature buncher cavity and two solenoidal lenses (see Fig. 1). The gun uses a GaAs photocathode driven by a Nd:YLF laser [3] . The drive laser is mode locked to

* Work supported by the Department of Defense under contract N00014-06-1-0587 with Northern Illinois University.

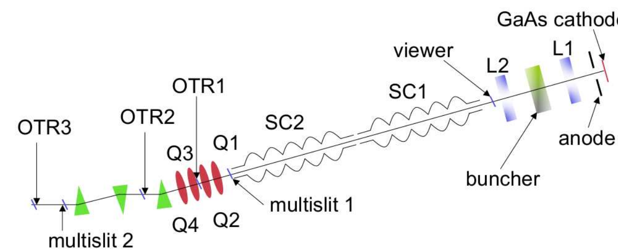

Figure 1: Overview of the Jlab IR-FEL photoinjector. The legend is "L1" "L2": solenoidal magnetic lenses, "SC1" "SC2" superconducting 5-cell CEBAF cavities, "Q1...4" quadrupoles, "OTR1...3" optical transition radiation screen, "multislit" emittance measurement stations. The green triangles indicate the locations of the sector dipoles composing the merger.

Table 1: Beam parameters specifications at the injection point ("multislit 2" in Fig. 1).

parameter	value	units
bunch charge Q	135	pC
transverse emit. $\varepsilon_{x,y}$	≤ 10	μm
$\beta_{x,y}$	10	m
$\alpha_{x,y}$	0	-
bunch duration $\sigma_t = \sigma_z/c$	[1.5,2.5]	ps
longitudinal emit. ε_z	≤ 28	ps-keV
energy spread σ_E	≤ 15	keV

37.425 MHz corresponding to the fortieth subharmonic of the rf fundamental frequency (1497 MHz) of the RF system. It can provide various micropulses shape and durations with a variable repetition rate ranging from 0.245 to 74.850 MHz. The gun is currently operated at 350 kV. Efforts to develop a gun capable of withstanding an accelerating voltage of 500 kV are underway. The beam is then ballistically bunched with a 1.5 GHz single-cell buncher [6] located $\sim$ 1 m upstream of the SCRF accelerating section. The accelerating section incorporate two modified CEBAF 5-cell cavities capable of maximum peak E-field of $\sim$ 20 MV/m.

The performance of the beam generation and acceleration section was investigated with ASTRA [7]. The dc-gun and the magnetic solenoid lenses are modeled by their axial electric or magnetic field obtained from POISSON simulations. The CEBAF cavities and buncher are described by their axial electric field simulated using SUPERFISH. In all the cases the electromagnetic structures are assumed to be cylindrical-symmetric and the radial electric and azimuthal magnetic fields are derived form a third order off-axis expansion. An evolutionary algorithm GENETICOPTIMIZER [8] was used in conjunction with ASTRA to seek a set of optimum operating parameters for the photoinjector such to minimize the longitudinal emittance downstream of the accelerating section. The transverse emittance, bunch duration, and energy spread were constrained accordingly to the specified range of values shown in Table 1. For fast throughput 2000 macroparticles were used to optimize the accelerator settings. The variable param-

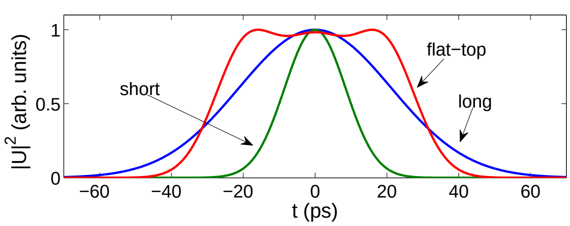

Figure 2: The three different photocathode drive laser intensity temporal distribution assumed for the optimization of the generation and acceleration section.

eters for the optimization were: the transverse laser spot size, the solenoids magnetic field, the buncher and accelerating cavities electric field amplitudes and phases. The photocathode drive laser was assumed to have a uniform cylindrically-symmetric transverse distribution and three cases of temporal distributions were considered (Fig. 2). The evolution of beam parameters obtained for the best longitudinal emittance are shown in Fig. 3 for the three cases of the laser temporal distributions shown in Fig. 2. These simulations were performed using 200k macroparticles. The "long" laser pulse does not meet the specified longitudinal emittance while the "short" and "flat top" shapes for the laser temporal distribution meet all requirements. The optimum settings for the short laser case call for a rather large laser spot size of $\sigma_c = 4$ mm (the maximum allowed – and twice of the spot size routinely used) on the photocathode. This, in turn, results in large transverse spot sizes in the low energy transport upstream of the accelerating cavities. However no particle loss are observed in our simulations (the beam pipe apertures are included). For these three sets of simulations the kinetic energy is within the specified range of $[9, 10]$ MeV.

10 MEV SECTION

The 10 MeV accelerating section is followed by a quadrupole telescope and a "staircase" achromatic merger composed of three sector bending dipoles with bending angles $\theta = (+, -, +)\ 20°$. The dispersion function reaches a maximum in the second dipole ($|\eta_x| \simeq 56.38$ cm) and has a value of $|\eta_x| = 30$ cm at OTR2

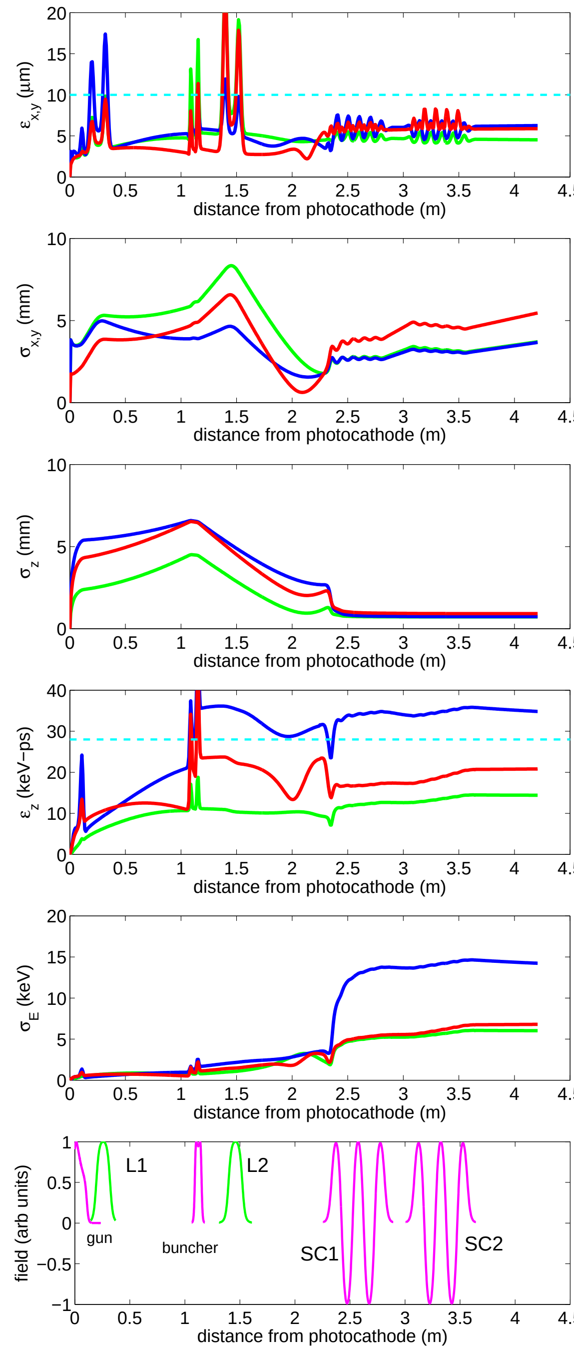

Figure 3: Rms beam parameters for the optimum injector settings that result in the smallest longitudinal emittance for the three different photocathode drive laser temporal distribution shown in Fig. 2 (same color coding is used). The bottom plot shows the field profile and location of each component. The symbols are defined in Table 1 and Fig. 1, $\sigma_{x,y}$ is the rms transverse beam size.

(see Fig. 1) thereby enabling energy profile measurement. The merger is non-isochronous with a longitudinal dispersion $R_{56} \simeq -19.25$ cm[1]. Therefore an incoming bunch with proper correlated energy spread can be further compressed. Two effects set the upper and lower limits on the bunch length downstream of the merger. On one hand a longer bunch length alleviates the detrimental effects of longitudinal space charge [10]. On another hand longer bunch lengths result in nonlinear (mainly quadratic) distortions of the longitudinal phase space as the bunch is accelerated in the downstream cryomodules. Such distortions yield significant longitudinal emittance growth. Simulations of the beam dynamics in the merger were

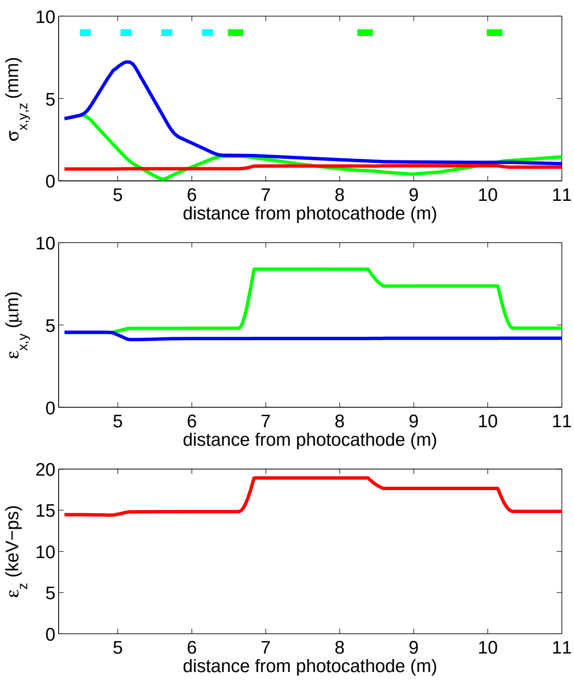

Figure 4: Rms beam properties along the 10 MeV section for the "short" laser pulse shape. The cyan and green rectangles on the upper plot respectively indicate the location of the quadrupoles and sector dipoles.

performed with IMPACT-T [11] which incorporates a 3-D poisson solver. Coherent synchrotron effects are neglected. The quadrupoles were varied to approximately achieve the desired Courant-Snyder parameters at the entrance of the main linac. The evolution of the rms beam parameters associated to the case of the short laser pulse shows minor emittances dilutions through the 10 MeV section; see Fig. 4. The corresponding longitudinal phase space at the injection point is shown in Fig. 5. Furthermore IMPACT-T simulations confirm that the bunch length can be tuned by varying the phase of SC2 without affecting the beam emittances (the final bunch length were $\sigma_z \in [0.5, 2]$ mm).

[1] In our matrix convention the $t > 0$ corresponds to the tail of the bunch

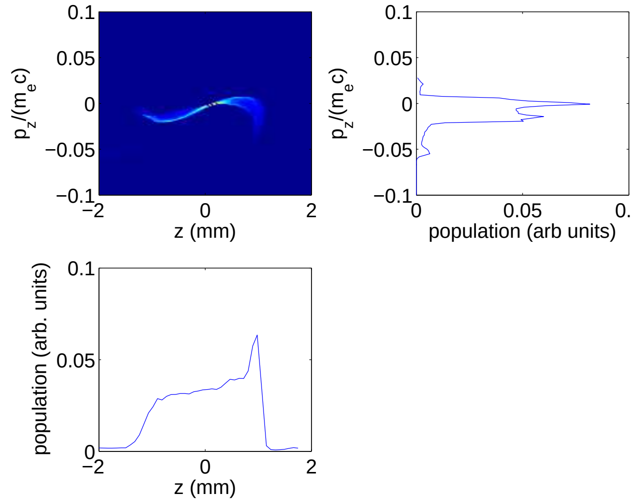

Figure 5: Longitudinal phase space and corresponding projections at the injection point for the "short" laser case.

SUMMARY

Simulation and optimization of the injector currently in operation at the 10 kW JLab FEL have been performed for different scenarios of photocathode drive lasers. Optimum settings were found for two laser configurations that could provide beam parameters within the specified values. It is hoped that these simulations will serve as guidance to test and validate new settings of the photoinjector aimed at lowering the longitudinal emittance.

REFERENCES

[1] S. V. Benson, *et al.*, Proceedings of the 2007 Particle Accelerator Conference, Albuquerque NM, 79 (2007).

[2] G. R. Neil, *et al.*, *Phys. Rev. Lett.*, **84**, 662 (2000).

[3] D. Engwall *et al.*, Proceedings of the 1997 Particle Accelerator Conference, Vancouver BC, 2693 (1997).

[4] H. Liu, D. Neuffer, Proceedings of the 1995 Particle Accelerator Conference, Dallas TX, 1867 (1995).

[5] P. Piot, *et al.*, Proceedings of the 1998 European Particle Accelerator Conference, Stockholm Sweden, 1447 (1998).

[6] B. C. Yunn, CEBAF internal report TN-94-021, available from Jefferson Lab (1994).

[7] K. Flöttmann, ASTRA: A space charge tracking algorithm, available from www.desy.de/~mpyflo/Astra_dokumentation

[8] M. Borland and H. Shang, GENETICOPTIMIZER unpublished program (private communication, 2006).

[9] C. Hernandez-Garcia et al., Proceedings of the 2004 FEL conference, Triestre Italy, 558 (2004).

[10] C. Hernandez-Garcia et al., Proceedings of the 2004 FEL conference, Triestre Italy, 363 (2004).

[11] The IMPACT-Z / IMPACT-T suite of codes was provided by Ji Qiang of LBNL (2007).